Oxidation Behaviour at 1100°C of HfC-Containing Co-Based Alloys

Patrice Berthod

Oxidation Behaviour at 1100°C of HfC-Containing Co-Based Alloys

Patrice Berthod[1,2,*]

[1]*Campus Victor Grignard, B.P. 70239, 54506 Vandoeuvre-lès-Nancy – France*

[2]*Campus ARTEM, 2 allée André Guinier 54000 Nancy– France*

Abstract: Cobalt alloys may be efficiently strengthened by hafnium carbides for uses at high temperature. However the presence of Hf in quantities high enough to allow significant creep-resistance may lead to particular behaviour in oxidation at high temperature. In this work three HfC-containing cobalt-based alloys were exposed to synthetic air at 1100°C for 50 hours, to observe their surface reactivity. The change in mass by oxidation, the general surface state, the oxide scales and subsurface changes specified by cross-sectional characterization were studied. They were compared to similar results obtained for hafnium-free cobalt alloys with the same chromium and carbon contents, considered as references. The presence of several weight % of hafnium obviously induced a real deterioration of the resistance against oxidation at 1100°C. This shows that these cobalt alloys must be improved for better resisting high temperature oxidation. This is compulsory to allow lifetime really benefiting from the mechanical strengthening brought by the HfC interdendritic network.

Keywords: Cobalt alloys, hafnium carbides, high temperature, oxidation, surface examination, cross-sectional metallographic investigations.

1. INTRODUCTION

Hafnium is essentially an element known for its beneficial effect on the high temperature oxidation and corrosion behaviour of superalloys [1,2]. But its influence may also concern the mechanical properties of structural materials [3]. The HfC carbides are particularly stable at high temperature in cast cobalt-based alloys [4]. However these carbides are almost never used for strengthen refractory alloys against mechanical stresses at high temperature, in contrast with other carbides such as chromium carbides, TaC… [5-7]. However recent results demonstrated that HfC carbides may lead to exceptional resistance against creep at elevated temperature [8]. They appear thus as possible very interesting alternative carbide-based strengthening systems for superalloys, serious challengers for chromium carbides [20] and MC carbides of other types [21-23].

The contents in Hf required to develop sufficiently dense HfC network in a cobalt-based alloy are much higher than when this is only the improvement in high temperature oxidation behaviour which is wished. Indeed, instead about 1wt.% which is commonly chosen, an efficient HfC carbides network needs several weight % in hafnium, which may totally transform the oxidation phenomena during uses at high temperature. To better know how alloys of this new generation of cobalt-based alloys behave at 1100°C in term of surface reactivity, three alloys were synthesized and tested in oxidation. Different content levels in hafnium and carbon were chosen for their chemical compositions. After oxidation test the surface and subsurface deteriorations were specified by post-mortem characterization.

2. EXPERIMENTAL DETAILS

Three Co-25wt.%Cr alloys containing various quantities of hafnium and carbon were elaborated under inert atmosphere (Ar, 300mbars). This was done using a High Frequency induction furnace (CELES, France). The targeted compositions were: Co-25Cr-0.25C-3.7Hf (“CHF1”), Co-25Cr-0.50C-3.7Hf (“CHF2A”) and Co-25Cr-0.50C-7.4Hf (“CHF2B”). To reveal the specific effect of the presence of hafnium, more precisely of the hafnium carbides, two alloys with the same chromium and carbon contents, but free of hafnium were also considered: the ternary Co-25Cr-0.25C (“C1”) and Co-25Cr-0.5C (“C2”) alloys. They were elaborated following the same route. All alloys were synthesized from pure elements (99.9wt.% of purity) and obtained as ingots weighing about 40 grams. The names of all these five alloys and their targeted compositions are gathered in Table **1**.

After cutting, parts of the obtained ingots were embedded in a cold resin mixture (ESCIL, France) and ground with SiC papers whose grade varied from 240-grit to 1200-grit. After ultrasonic cleaning, final polishing was achieved using a textile disk enriched with fine hard particles until obtaining a mirror-like surface. The as-cast microstructures were examined using a JEOL JSM-6010LA Scanning Electron Microscope (SEM) in

*Address correspondence to this author at the Campus Victor Grignard, B.P. 70239, 54506 Vandoeuvre-lès-Nancy – France; Tel : (+33) 383684666 ;
E-mail: patrice.berthod@univ-lorraine.fr

E-ISSN: 2410-4701/17

Table 1: Designation and Targeted Compositions in wt.% of the Five Studied Alloys

Alloys Weight Contents	C1	CHF1	C2	CHF2A	CHF2B
Co	Bal.	Bal.	Bal.	Bal.	Bal.
Cr	25	25	25	25	25
C	0.25	0.25	0.50	0.50	0.50
Hf	/	3.7	/	3.7	7.4

Back Scattered Electron mode (BSE). The general compositions of the alloys (except carbon) were controlled by Energy Dispersion Spectrometry (EDS).

In each ingot, another part, which was devoted to the oxidation exposure, was also cut: a parallelepiped of about 3mm × 8mm × 8mm. Edges and corners of these parallelepipeds were smoothed with 240-grit SiC paper before the sample was all around ground with 1200-grit SiC paper. The obtained sample was measured (0.01-precision electronic caliper), weighed (0.0001g-precision microbalance), then placed in the hot zone of a tubular resistive furnace (SETARAM, France). The applied thermal cycle was composed of a +20 K/min heating, a 50 hours stage at the constant temperature of 1100°C, and of a -5K/min cooling down to room temperature. The oxidized samples were weighed again. Photographs were taken on the main oxidized surfaces (both sides) using a simple office scanner, and X-ray diffraction was carried out using a Philips X'Pert Pro diffractometer. This aimed to have a look to the oxide spallation state and to specify representatively the natures of the oxides over a greater surface than possible by SEM.

Cross-sectional examinations of the oxide scales and of the subsurfaces were carried out using the SEM. For that the oxidized samples were thereafter coated by gold (cathodic pulverization) to give good electrical conductivity to the external surface. Thereafter a thick nickel shell was electrolytically deposited in a 50°C-heated Watt's bath under 1.6A/dm², for protecting the external oxide scales from the mechanical stress which will be induced by cutting. The Ni-coated samples were then sectioned using a precision saw. The obtained halves were embedded, ground and polished as described above for the as-cast samples. The oxides were characterized by SEM/BSE imaging and by EDS spot analysis. Successive EDS spot analyses were carried out from the oxide/alloy interface inward the bulk, perpendicularly to the external surface. This will allow having a look to the local chemical composition evolution, notably to the chromium depletion.

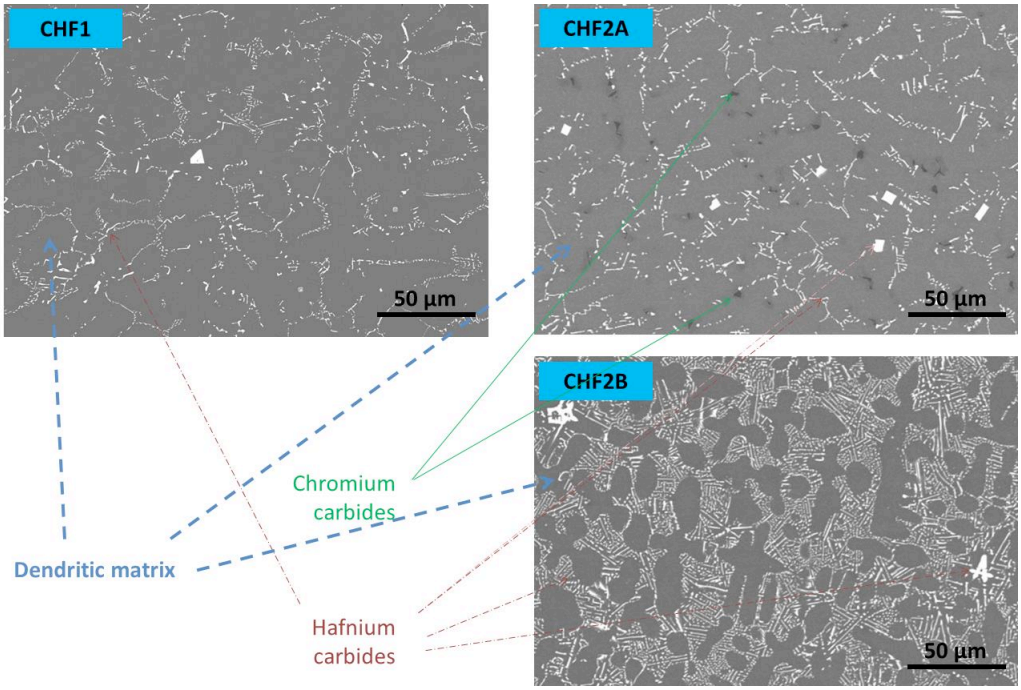

Figure 1: Microstructures of the three Hf-containing Co-based alloys (SEM, BSE mode).

3. RESULTS AND DISCUSSION

3.1. As-Cast Microstructures

The microstructures of the three Hf-rich cobalt-based alloys are illustrated in Figure **1** by SEM/BSE micrographs. The matrix of each of them is dendritic and the interdendritic spaces are occupied by white particles. EDS spot analyses showed that these ones are HfC carbides. These carbides are almost as numerous in the CHF1 alloy as in the CHF2A one, while they are significantly more present in the CHF2B alloy. Obviously the HfC population is monitored by the Hf content, provided that there are carbon atoms enough to allow employing all Hf atoms in HfC carbides. This is obviously the case for these alloys since the Hf/C weight contents ratios chosen for these alloys correspond to the atomic ones equal to 1 for the CHF1 and CHF2B alloys, while the one for the CHF2A alloy corresponds to a Hf/C atomic ratio equal to 0.5.

Thus the whole hafnium is involved in the formation of HfC carbides, as proven by spot analyses performed in the matrix which showed that there is no Hf in solid solution. This demonstrates the exceptionally strong carbide-former character of hafnium. Because it contained twice more carbon atoms than hafnium atoms, the CHF1 alloy also contains chromium carbides (dark particles which are also present in the interdendritic spaces).

The HfC carbides are mainly elongated (CHF1 and CHF2A alloys) or script-like (CHF2B) but some of them are also blocky particles. These ones probably crystallized early during solidification (pre-eutectic carbides) while the others clearly precipitated at the end of solidification by forming a eutectic compound with matrix.

The two ternary alloys, the as-cast microstructures of which are not illustrated here because being too classical, are simply composed of a dendritic solid solution and of interdendritic chromium carbides, logically more present in the C2 alloy than in the C1 alloy.

3.2. Global Aspect of the Oxidized Samples and XRD Results

After the {1100°C, 50 hours}-oxidation runs, all the five samples were covered by an external oxide layer. However the scales have obviously spalled off during the cooling since the alloys are here and there denuded (Figure **2**). This oxide spallation was simply quantified by mass variations.

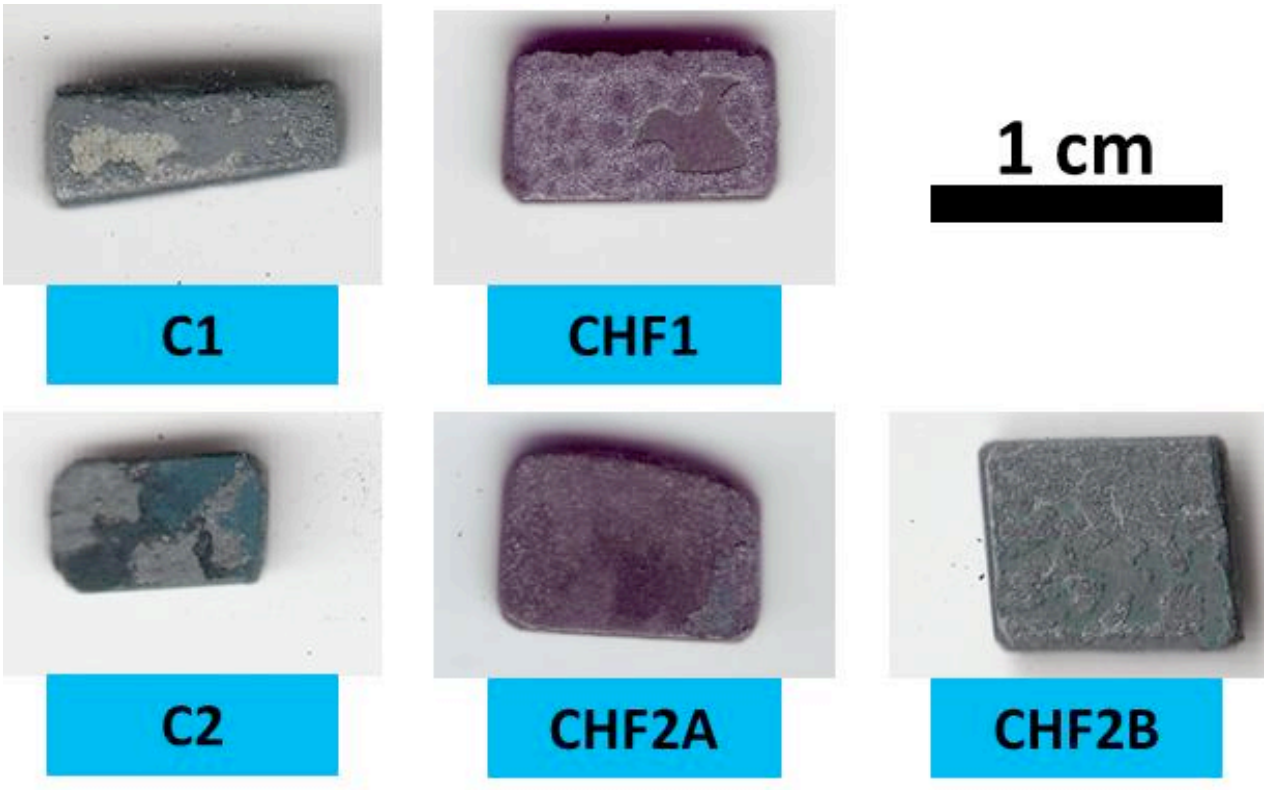

Figure 2: Global view of the surface states of the samples after the oxidation test (office scanner).

Table 2: Total Mass Variation During the Whole Thermal Cycle, for the Five Alloys

Alloys	C1	CHF1	C2	CHF2A	CHF2B
Surface (cm²)	1.6159	1.4083	1.0194	1.4997	1.7389
m before (g)	0.8491	0.5570	0.3383	0.5204	0.8395
m after (g)	0.8456	0.5580	0.3333	0.5127	0.8467
m diff (g)	-0.0035	+0.0010	-0.0050	-0.0077	+0.0072
m/S diff (g/cm²)	-0.0022	+0.0007	-0.0049	-0.0051	+0.0041

Table 3: Total Mass Variation During the Whole Thermal Cycle, for the Five Alloys

Alloys oxidized at 1100°C	CoO	$CoCr_2O_4$	Cr_2O_3	HfO_2
C1	**YES**	**YES**	**YES**	**NO**
CHF1	**YES**	**YES**	**YES**	**NO**
C2	**YES**	**NO**	**YES**	**NO**
CHF2A	**NO**	**YES**	**YES**	**YES**
CHF2B	**YES**	**YES**	**YES**	**YES**

These results, displayed in Table **2**, confirm what was deduced from the views given in Figure **2**: spallation occurred for the five alloys, of similar magnitude, independently on the Hf presence.

Nevertheless the scales were still present in quantities high enough to allow identifying the natures of oxides by XRD, prior to cross-sectional observations. As shown in Table **3** none of the five alloys is really chromia-forming. Chromia is detected but other oxides also formed, as the cobalt oxide CoO and the spinel oxide $CoCr_2O_4$. For the Hf-rich alloys the hafnium oxide HfO_2 additionally formed.

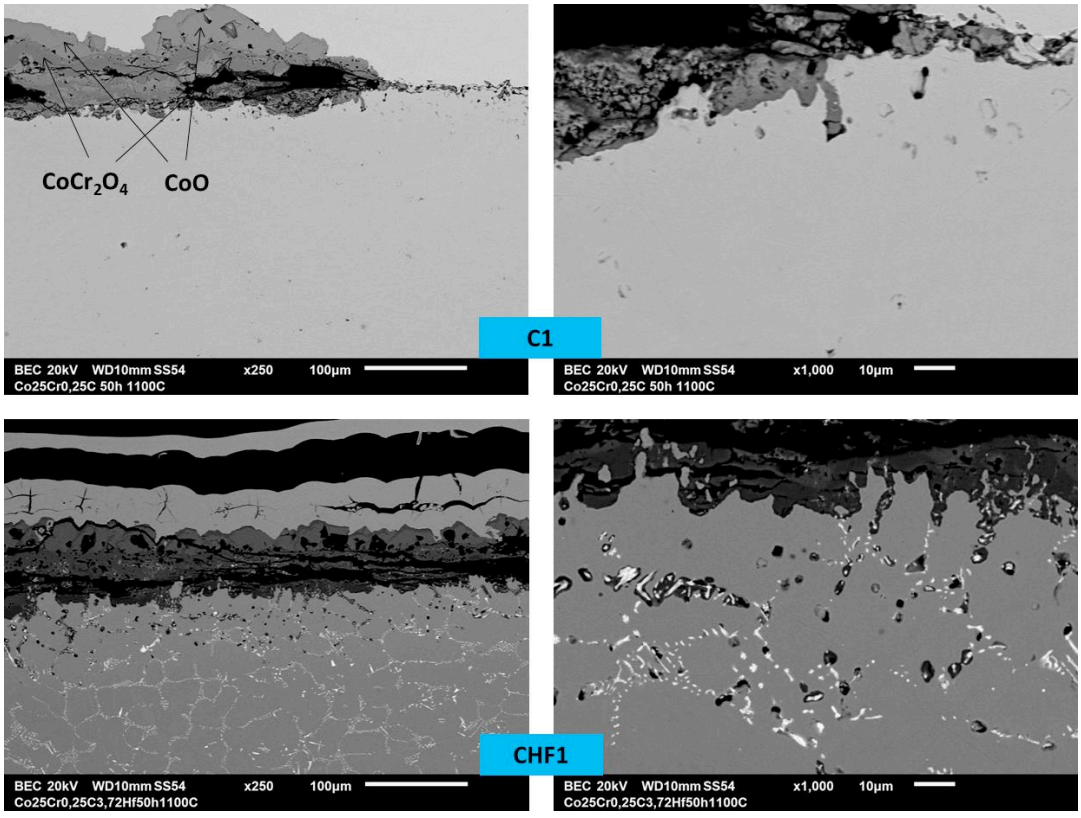

Figure 3: Surface and subsurface states of the two 0.25C-containing alloys (SEM, Back Scattered Electrons mode); general view (left) and detailed view (right).

3.3. SEM/EDS Cross-Sectional Characterizations

After the preparation of cross-sectional samples the oxide scales and sub surfaces were examined by SEM in BSE mode. The surface and subsurface states of the two 0.25C-containing alloys (C1 and CHF1) after oxidation are illustrated for two magnifications in Figure **3**, while the surface and subsurface deteriorations of the three oxidized 0.50C-containing alloys (C2, CHF2A and CHF2B) are illustrated in Figure **4**.

The CoO, $CoCr_2O_4$, Cr_2O_3 and HfO_2 oxides are well distinguished by the BSE mode, thanks to different grey levels. The cobalt oxide (rather clear) is dense and it often constitutes the most external part of the external scale. In contrast chromia, which is the darkest oxide present, is also rather dense but often located close to the alloy, as is to say it is the most internal part of the scales. The spinel oxide, intermediate grey level, is generally porous. The hafnium oxide (CHF1, CHF2A and CHF2B alloys only) is the white one. It is less present than the formers, and dispersed as islands mixed with chromia or with the spinel oxide.

It seems that the oxidation progress was twice: outward (CoO) by cationic diffusion (Co^{2+}) and inward ($CoCr_2O_4$ and Cr_2O_3 with presence of HfO_2) by anionic diffusion (O^{2-}). Indeed, besides places where the

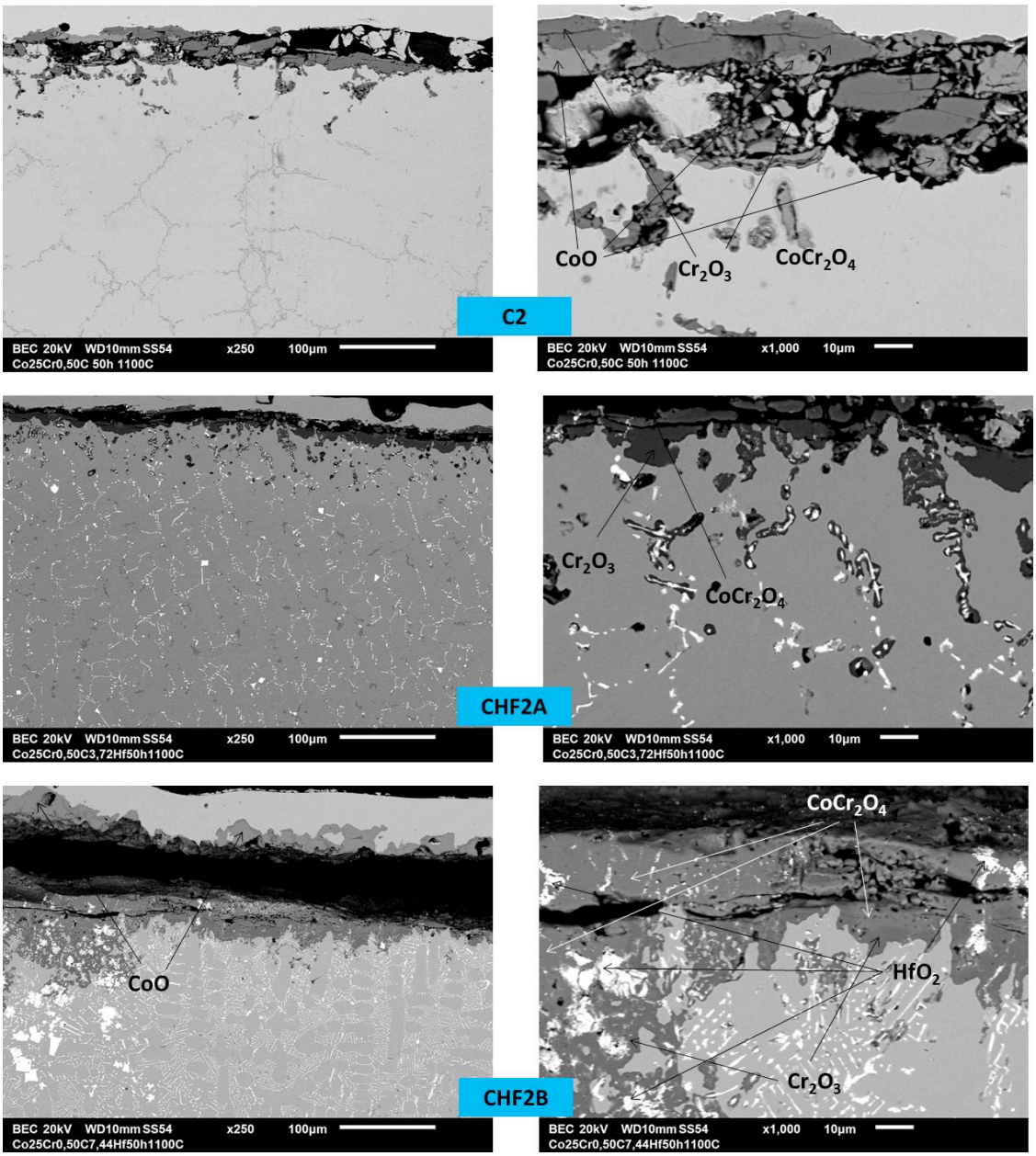

Figure 4: Surface and subsurface states of the three 0.50C-containing alloys (SEM, Back Scattered Electrons mode); general view (left) and detailed view (right).

Table 4: Chromium Contents in Extreme Surface (Average and Standard Deviation Calculated from Five Results); EDS Spot Analysis

Elements in extreme surface	Average wt.%Cr	Std deviation wt.%Cr
C1	13.08	4.08
CHF1	8.21	2.24
C2	13.94	1.66
CHF2A	12.95	0.54
CHF2B	17.59	1.20

oxide/alloy interface is straight (example: right side of the top-left micrograph of Figure **3**, external scale only, lost by spallation), there are other places which are irregularly hollowed (left side of the same micrograph, inner chromia and spinel oxides having resisted spallation since trapped here).

One can also notice that the HfC carbides did not dissolve from the oxidation front (as chromium carbides or tantalum carbides do in other cast carbides-strengthened alloys) but staid stable or transformed *in situ* as oxides.

The chemical compositions in alloy were specified close to the oxide/alloy by spot EDS analyses. The results concerning chromium, displayed in Table **4**, show that its content has fallen at rather low levels in all cases. The Hf contents are the most often equal to zero, as anywhere in the bulk.

Some EDS concentrations profiles were performed inward perpendicularly to the surface, from the oxide/alloy interface (Figure **5**). They reveal severe chromium depletion over a depth of about 50µm. This rather thin Cr-depleted subsurface zone and the apparent high value of the Cr content gradient let think to a difficult diffusion of Cr. This may be attributed to an

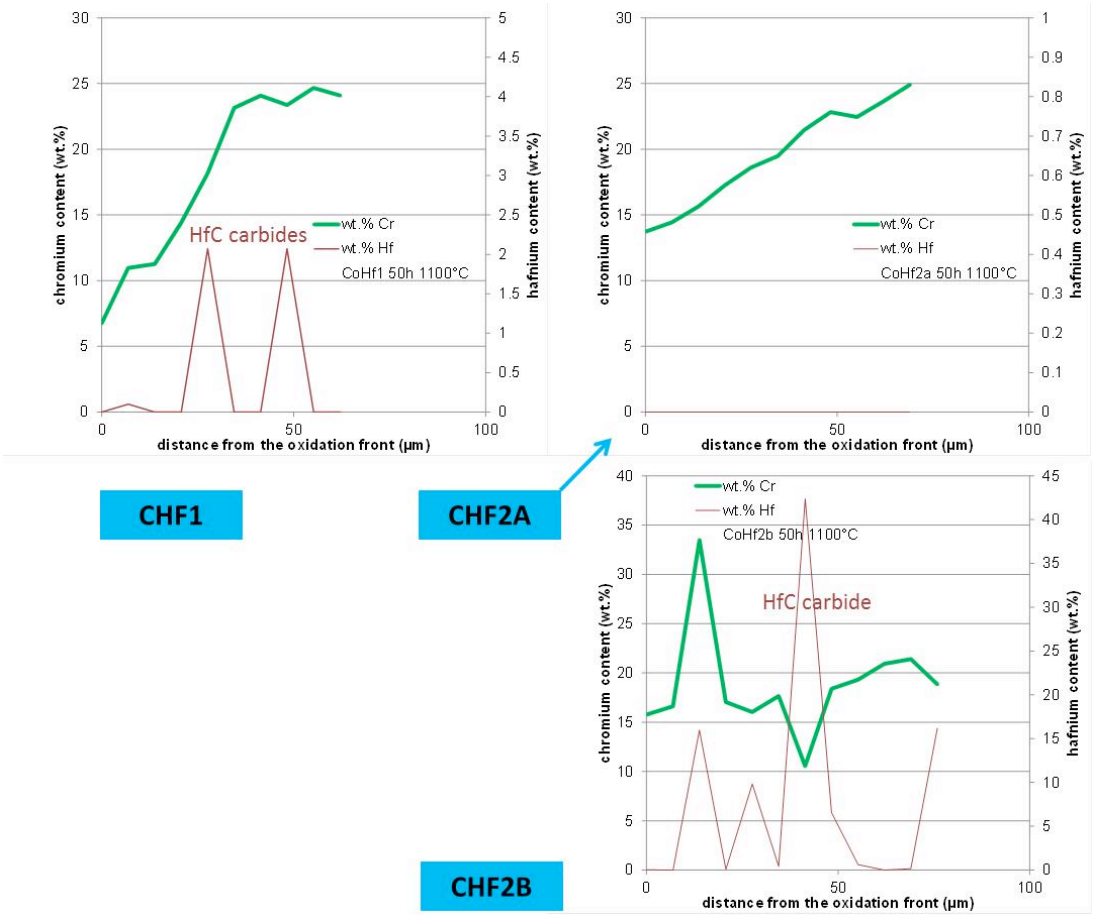

Figure 5: Concentrations profiles acquired by EDS from the oxide/alloy interface.

obstruction of the Cr mobility in the interdendritic boundaries by the HfC and HfO_2 particles which stayed here.

This apparently obstructed diffusion of the Cr atoms in the grain boundaries, which is an important mode of Cr supplying mean for the oxidation front at this temperature of 1100°C. Indeed this temperature is high but not enough to give an important role to the diffusion in volume. This probably posed a serious problem for the oxidation resistance of the studied Hf-rich alloys. It was already true that the base of these alloys, simulated by the ternary alloys, was not really favored because of a cobalt-base matrix (less efficient for Cr diffusion in volume than a nickel-based one) and of an initial chromium content in alloy not very high. But the additional presence in the interdendritic spaces of obstacles for Cr diffusion (initial HfC and later formed HfO_2) in the Hf-rich alloys aggravated the situation. The low chromium contents in alloy in extreme surface and the multiplicity of oxides formed (not only chromia) with here and there deep oxidation penetration in alloy, demonstrated that the behaviors of the alloys were not chromia-forming and that oxidation threatened to be soon catastrophic.

CONCLUSIONS

The HfC-strengthened alloys, whose oxidation behaviours were studied at 1100°C here, are clearly not resistant enough to the aggressiveness of hot air. Despite their superior creep-resistance at high temperature, the lifetime of pieces made of these alloys will be without any doubt severely shortened by chemical destruction. Indeed this started before only fifty hours here. A possible detrimental role of the HfC carbides was pointed out: obstruction of the interdendritic chromium diffusion. It is clear that such alloys cannot be used in their present state for the hottest parts of the aeronautic or energy generation turbine blades or for the tools working at elevated temperature in some industrial applications in which high temperature chemical aggressions act as well as mechanical stresses. Among the possible solutions for improving the oxidation resistance of such alloys one can mention first choosing a higher chromium content for the whole alloys. But it may be preferable to enrich the surface and subsurface in chromium, for example by pack-cementation, in order to do no oblige chromium to diffuse from the bulk. Future works can be devoted to the exploration of this solution.

ACKNOWLEDGEMENTS

The author would like thank very much Thierry Schweitzer, Elodie Conrath and Pascal Villeger for their practical contributions to this work.

REFERENCES

[1] Young J. High Temperature Oxidation and Corrosion of Metals. Elsevier, Amsterdam 2008.

[2] Stringer J, Allam IM and Whittle DP. Thin Solid Films 1977; 45(2): 377. https://doi.org/10.1016/0040-6090(77)90273-5

[3] Maksyuta II, Koatyrko OS, Pedan TN and Baturinskaya NL. Nov v Litein Pr-ve, Kiev 1981; 103.

[4] Berthod P. Journal of Alloys and Compounds 2009; 481(1-2): 746. https://doi.org/10.1016/j.jallcom.2009.03.091

[5] Lobl K. Cobalt 1968; 38: 29.

[6] Donachie MJ and Donachie SJ. Superalloys: A Technical Guide – 2nd Edition', ASM International. Materials Park 2002.

[7] Berthod P, Bernard JL and Liebaut C. patent WO 2001090429 A1 20011129.

[8] Berthod P and Conrath E. Journal of Materials Science and Technology Research 2014; 1(1): 7. https://doi.org/10.15377/2410-4701.2014.01.01.2

[9] Li Z, Mao H and Selleby M. Calphad 2017; 59: 107. https://doi.org/10.1016/j.calphad.2017.09.002

[10] Liu Y, Jiang Y, Zhou R and Feng J. Journal of Alloys and Compounds 2014; 582: 500. https://doi.org/10.1016/j.jallcom.2013.08.045

[11] Shu DL, Tian SG, Tian N, Xie J and Su Y. Materials Science and Engineering A 2017; 700: 152. https://doi.org/10.1016/j.msea.2017.05.108

[12] Zhang L, Liu H, He X, Din R, Qu X, et al. Materials Characterization 2012; 67: 52. https://doi.org/10.1016/j.matchar.2012.02.014

Received on 07-12-2017 Accepted on 15-12-2017 Published on 31-12-2017

DOI: http://dx.doi.org/10.15377/2410-4701.2017.04.2